Analytical Iterative Multistep Interval Forecasts of Wind Generation Based on TLGP

Juan Yan, *Member, IEEE*, Kang Li, *Senior Member, IEEE*, Erwei Bai, *Fellow, IEEE*, Xiaodong Zhao, Yusheng Xue, and Aoife M. Foley, *Member, IEEE*

Abstract—Probabilistic wind power forecasting has become an important tool for optimal economic dispatch and unit commitment of modern power systems with significant renewable energy penetrations. Ensemble forecasting based on Monte Carlo simulation has been widely adopted by grid operators, but other probabilistic approaches, such as multistep iterative wind power forecasting have not yet been fully explored. The associated uncertainty analysis is an important yet challenging issue in this area. This paper proposes to use an analytic interval forecasting framework to estimate the forecasting uncertainty and its propagation with multisteps for two wind farms based on the temporally local Gaussian process (TLGP) model. The key findings confirm that TLGP forecasting not only has better accuracy but is also more reliable and sharp than other benchmark models. This paper provides an innovative analytical framework for iterative multistep interval forecasts.

Index Terms—Probabilistic forecasting, gaussian process, uncertainty propogation, wind energy.

NOMENCLATURE

The key symbols used in the paper are defined below for quick reference while others are defined after their first appearance as required.

x	Deterministic input (state vector).
(X, Y)	Available training dataset.
θ^*	Optimal hyperparameters.
B, B_t	Cross-covariance vector.
C_Y, C_t	Covariance matrix.
$\mu(x)$	Mean function of prediction under x.
$\sigma^2(x)$	Variance function of prediction under x.
Φ	Covariance function.
x^*	Column vector of random input.
μ_{x^*}	Expectation of x^*.
Σ_{x^*}	Covariance matrix of x^*.
$m(x^*)$	New mean output under random input x^*.
$v(x^*)$	New variance of output under random x^*.
$E_{x^*}[f]$	Expectation of f under x^*.
$Var(\cdot)$	Analytical definition of variance.

I. INTRODUCTION

ACCURATE wind power forecasting plays a key role in modern power systems to mitigate the impacts of the stochastic and variable nature of wind energy [1], [2]. Probabilistic forecasting has been widely used in the research of energy storage [3], reserve quantification [4], unit commitment and market trading [5]. In [6], probabilistic forecasting was used to estimate dynamic operation reserve requirements based on the uncertainty information in each forecasting interval. It was found that probabilistic wind power forecasting, together with a proper demand dispatch plan, can contribute significantly to the efficient and economic operation of electricity markets and improve unit commitment. In [7], optimal bidding strategies were developed based on the probabilistic forecasting and sensitivity modelling, which increase revenues for stakeholders and maximize the benefits of wind power generation. In [8] it was shown that the uncertainty assessment of wind power prediction using local quantile regression benefits the grid operations when incorporated in real-time energy management systems.

Machine learning methods have been used in probabilistic wind power forecasting including the parametric methods such as extreme learning machine (ELM) [9], sparse vector autoregressive (sVAR) 0, fuzzy neural networks 0 and the nonparametric method such as the adaptive resampling 0. The evaluation metrics of probabilistic forecasting have been defined including reliability, sharpness and the unique skill score 0. There are several typical forms of probabilistic forecasting: 1) probability distribution function (p.d.f) and cumulative distribution function (c.d.f.); 2) quantiles and intervals; 3) discrete probabilities; 4) moments of probability distribution [14]. Among them, interval forecasts give a range of intervals within which the observed

variable is expected to fall in with the pre-defined probabilities. The current interval forecasts techniques include empirical error based methods, such as the parametric method [15] which assumes the shape of error distribution and the nonparametric method [12] which does not. Both kinds of empirical approaches assume that future uncertainty can be expressed from the recently witnessed behavior of the point prediction method and the error of point forecasting are employed for further analysis. However, the resulted confidence intervals do not necessarily cover the measurements, which is not in favor of the above assumption. The other type of interval forecast is the direct interval forecast [16]–[17]. The intervals are given without the prior knowledge of forecasting errors. In [16], the prediction intervals and the corresponding confidence levels are predicted by directly optimizing the reliability and sharpness with Extreme Learning Machine based methods. Only time series wind generation data is employed for 90%, 95% and 99% interval forecasts to ensure computational efficiency for hourly ahead forecasting. In [17], the direct interval forecast is developed based on neural networks for 4 fixed very short-term horizons with a confidence probability of 90%. However, these methods train the model separately for multi-horizon point forecasting and bring in additional complex computation in the multi-horizon interval forecasts. Therefore, an iterative way of implementing the probabilistic interval forecasts becomes necessary in terms of efficiency. This paper proposes an iterative interval forecast method based on a variant of Gaussian Process. It analyses how the uncertainty propagates and accumulates with iterative multi-step forecasting for the first time and the analytical expression of the uncertainty for each prediction horizon is derived. The results are evaluated and compared with other benchmark models. Considering the computing-efficiency of the iterative forecasting, this TLGP based interval forecast will benefit the real-time power system operation and management due to its high accuracy, reliability and efficiency.

TLGP is a non-parametric method proposed to adapt to the time-varying characteristic of the wind power forecasting, to enhance the local forecasting accuracy of the Gaussian Process (GP) and to reduce the computational demand [18]. Moreover, TLGP like GP generates not only the mean value of the prediction for a certain horizon but also the variance representing the uncertainty of the new prediction. In other words, it provides the prediction intervals with the lower and upper bound and the pre-defined probability of falling in the interval. TLGP is naturally tuned for interval forecasts.

For multistep forecasting, the iterative method estimates the next wind output and employs that estimate for the further forecasting step. It eliminates intensive re-computation, reducing the computational time and thus increasing the efficiency [19]. The relevance of uncertainty propagation in interval forecasting using iterative multi-step forecasting for more accurate wind power forecasting is studied with a case study of a wind farm in Ireland. The results are then evaluated using two metrics, namely reliability and sharpness, for probabilistic predictions in wind power forecasting [13].

The remainder of the paper is organized into six sections. Section II introduces the framework of analytical interval fore-casting using the TLGP. Section III develops the uncertainty propagation for iterative multi-step TLGP under random inputs. Section IV presents the results and analysis of a case study. Section V discusses the probabilistic evaluations considering the case study and Section VI concludes the paper. The Appendix provides the Taylor expansion used to estimate the mean value and the variance under a random input.

II. ANALYTICAL INTERVAL FORECASTS WITH TLGP

There has been a lot of debates over the shape of the predictive error distribution and the correct assumptions to make for the wind power forecasting. In [20], Numerical Weather Prediction (NWP) method was used to predict wind speed first, and the wind power was obtained through the wind turbine power curve. It was widely recognized that the conditional distribution of wind power forecasting errors based on weather condition and wind speed follows strongly a non-Gaussian distribution due to the transformation of the wind speed to wind power, though in [21], Gaussian distribution was used to represent the wind power forecasting error for systems with significantly installed wind capacity, and a new approach was proposed to quantify the demand. In [22] the authors employed a persistence model for wind power forecasting and found that the predictive error was too fat-tailed to be Gaussian, and Beta distribution was used to fit the probability distribution. An energy storage system was designed to reduce the uncertainty. In [23], a generalization of the logit-Normal distribution was introduced in auto regression (AR) based models to describe the double-bounded nature of wind power. However, it should be noted that two variables are discussed above, namely the predictive error and the wind generation output. Generally speaking, the global distribution of the wind power generation is too skewed to be Gaussian empirically, and the global forecasting error based on the wind turbine working curve would not be Gaussian either.

The Gaussian Process assumes Gaussian noise in the observations [24], the non-linear relationship between the wind speed and the resultant wind power implies that this assumption may no longer be valid. However, the wind turbine working curve can be approximated by a series of piecewise linear segments and for each linear segment of the working curve, a Gaussian Process can be assumed. Thus, the wind power dynamics can be modelled by multiple local Gaussian Processes. The original local Gaussian Process was proposed in [25] where the local data within the Euclidean space are employed for local regression. For time series wind power forecasting where the system exhibits strong time-varying features and most recent measurements are mostly correlated to the following short-term generations, the TLGP proposed in [18] where the temporally local data within a moving window are utilized for short-term wind power forecasting, has shown to have a superior performance in comparison with existing approaches. Within the short moving window, the wind turbine working curve will exhibit linear property rather than a nonlinear one, thus the temporally local Gaussian Process is well applicable for such situations. For the scenarios where the wind power generation changes dramatically and a ramping event occurs, then a hybrid method

combining the most recent measurements and the similar historical data has been proposed [26]. The statistical analysis of the forecasting errors in the form of kurtosis and skewness of the distributions showed that TLGP generates the most Gaussian-like uncertainties in comparison with other benchmark models [18]. It is worth noting that the Gaussian assumption in time series forecasting has been widely used in the literature. In [9], [27], it has been demonstrated that even if the actual error distribution is non-Gaussian, the time series models based on Gaussian distribution assumption can still be applied with satisfactory performance. Further, the work of [21] uses Gaussian distribution of forecasting error for demand quantify and produces satisfactory performance. This paper mainly focuses on the uncertainty propagation of the TLGP for multi-step iterative forecasting, aiming to provide another innovative way for reliable interval forecasts of wind power generation.

For a wind power system, denote $y_k|_{k=1}^N$ as the kth measurement of the available generation output sequence, and $\boldsymbol{x}_k$ as the corresponding state vector for the time series model which is made up of the previous wind power generation data, then

$$y_k = f(\boldsymbol{x}_k) + v_k \tag{1}$$

where v_k is a random noise with $v_k \sim N(0, \ v_0)$. The objective of wind power forecasting is to predict the output y_t at time t based on available historic datasets (X, Y). According to Rasmussen [24], Gaussian Process could be derived for a system with the Gaussian noise in (1) based on the Bayesian inference. For the TLGP used in this work, it breaks the overall forecasting range into temporal regions and adapts to the time-varying characteristic of the wind power generations. The proposed TLGP proposed dynamically uses a set of local Gaussian Process models to approximate the process with nonlinear noise. Locally the process is modelled as a Gaussian process, though the global function can be far from Gaussian. The amplitude and the distribution analysis of forecasting errors in [18] has verified the effectiveness of this model.

Gaussian Process makes new probabilistic prediction in (2) where A, B and C_Y are covariance between variables. It gives the mean value of the new prediction as well as the uncertainty associated in terms of variance. One of the most popular covariance functions is shown in (3) where v_1, v_0, and ω_d represent each element of the hyper-parameter vector θ, and δ_{ij} is the Kronecker delta function.

$$P(y_t|Y, X, \theta^*, \boldsymbol{x}_t) = N\left(BC_Y^{-1}Y, \ A - BC_Y^{-1}B^T\right) \tag{2}$$

$$\mathrm{cov}(y_i, y_j) = \Phi(\boldsymbol{x}_i, \boldsymbol{x}_j)$$

$$= v_1 \exp\left(-\frac{1}{2}\sum_{d=1}^D \omega_d(\boldsymbol{x}_i(d) - \boldsymbol{x}_j(d))^2\right) + v_0 \cdot \delta_{ij} \tag{3}$$

The 'moving window' forecasting technique as shown in (4)–(9) was employed in TLGP, where t represents the time instants of prediction. Similar to GP, TLGP not only generates the mean value of prediction in (4), but also provides the variance/uncertainty of the prediction for one-step ahead forecasting in (5).

$$\hat{y}_t = \mu(\boldsymbol{x}_t) = B_t C_t^{-1} Y_t = B_t C_t^{-1} \begin{pmatrix} y_{t-1} \\ y_{t-2} \\ \vdots \\ y_{t-M} \end{pmatrix} \tag{4}$$

$$\sigma^2(\boldsymbol{x}_t) = A_t - B_t C_t^{-1} B_t^T \tag{5}$$

$$B_t = (\Phi(\boldsymbol{x}_t, \boldsymbol{x}_{t-1}), \Phi(\boldsymbol{x}_t, \boldsymbol{x}_{t-2}), \ldots, \Phi(\boldsymbol{x}_t, \boldsymbol{x}_{t-M})) \tag{6}$$

$$C_t = \begin{bmatrix} \Phi(\boldsymbol{x}_{t-1}, \boldsymbol{x}_{t-1}), \ldots, \Phi(\boldsymbol{x}_{t-1}, \boldsymbol{x}_{t-M}) \\ \vdots \quad \ddots \quad \vdots \\ \Phi(\boldsymbol{x}_{t-M}, \boldsymbol{x}_{t-1}), \ldots, \Phi(\boldsymbol{x}_{t-M}, \boldsymbol{x}_{t-M}) \end{bmatrix} \tag{7}$$

$$A_t = \Phi(\boldsymbol{x}_t, \boldsymbol{x}_t) \tag{8}$$

$$\boldsymbol{x}_{t-i} = (y_{t-i-1}, y_{t-i-2}, \ldots y_{t-i-L})^{\mathrm{T}} \tag{9}$$

Usually, non-parametric methods avoid assuming the type of new probabilistic distribution, however, this GP based algorithm makes use of the noisy time series generation and assumes the joint distribution between them. The new prediction is noisy-correlated to the previous measurement. Therefore, it becomes natural and possible for the new prediction to automatically follow Gaussian distribution. Under such circumstances, the three prediction intervals become apparent: Interval I $(\mu - \sigma, \ \mu + \sigma)$, Interval II $(\mu - 2\sigma, \ \mu + 2\sigma)$ and Interval III $(\mu - 3\sigma, \ \mu + 3\sigma)$, with the nominal probability of 68%, 95% and 99.7%, respectively. Therefore, three nominal proportions are naturally given without quantile definition. As in (5), the uncertainty can be analytically expressed, leading to a framework of analytical interval forecasting. It should be noted that here every new prediction has its individual uncertainty/variance, which is different from the statistical analysis over all the forecasting error.

The assumption of Gaussian distribution for TLGP has been validated in TLGP [18]. The principles and properties for probabilistic iterative multi-step forecasting are further derived, evaluated and compared with standard Gaussian distribution in this work.

III. Multistep Probabilistic Iteration Under a Random Input

A. Probabilistic Estimation for Random Inputs

Technically speaking, the model input $\boldsymbol{x}^*$ (state vector) of wind power prediction at time *t*, which is often made of previous measurements or previous predictions is assumed to be a random variable following a Gaussian distribution $\boldsymbol{x}^* \sim N(\mu_{\boldsymbol{x}^*}, \Sigma_{\boldsymbol{x}^*})$ and white noise v_0 is presented in the measurements. The uncertainty associated with the randomness is propogated in the new wind power prediction. In particular, in iterative multi-step prediction, the new estimation will be utilized for the next step prediction. Thus such uncertainty is accumulated in each step and can not be ignored.

Inspired by the method used in [28], the new variance and mean under a random input could be obtained by Talor

expansion which is derived in the Appendix and shown as follows:

$$m\left(\boldsymbol{x}^*\right) = \mu\left(\mu_{\boldsymbol{x}^*}\right) \tag{10}$$

$$v\left(\boldsymbol{x}^*\right) = \sigma^2\left(\mu_{\boldsymbol{x}^*}\right) + \mathrm{Tr}$$

$$\left\{ \Sigma_{\boldsymbol{x}^*} \left(\frac{1}{2} \left. \frac{\partial^2 \sigma^2\left(\boldsymbol{x}^*\right)}{\partial \boldsymbol{x}^* \partial(\boldsymbol{x}^*)^{\boldsymbol{T}}} \right|_{\boldsymbol{x}^*=\mu_{\boldsymbol{x}^*}} \right.\right.$$

$$\left.\left. + \left.\frac{\partial \mu_{\boldsymbol{x}^*}}{\partial \boldsymbol{x}^*}\right|^{\mathrm{T}}_{\boldsymbol{x}^*=\mu_{\boldsymbol{x}^*}} \left.\frac{\partial \mu_{\boldsymbol{x}^*}}{\partial \boldsymbol{x}^*}\right|_{\boldsymbol{x}^*=\mu_{\boldsymbol{x}^*}} \right) \right\} \tag{11}$$

where $m(\boldsymbol{x}^*)$ is the new mean output under random input $\boldsymbol{x}^*$, and is calculated by the mean $\mu()$ defined in (4) and $v(\boldsymbol{x}^*)$ is the new variance of output under random input $\boldsymbol{x}^*$, which includes a new term in comparison with (5). The calculation of (11) depends on the derivitives of the expected mean and variance prediction for TLGP, as shown in (12) and (13). Such uncertainty propagation rules under a random input apply the same to GP.

$$\frac{\partial \mu_{\boldsymbol{x}^*}}{\partial \boldsymbol{x}^*_d} = \frac{\partial B\left(\boldsymbol{x}^*\right)}{\partial \boldsymbol{x}^*_d} C_{Y_t}^{-1} Y_t \tag{12}$$

$$\frac{\partial^2 \sigma^2\left(\boldsymbol{x}^*\right)}{\partial \boldsymbol{x}^*_d \partial \boldsymbol{x}^*_e} = -2 \frac{\partial B\left(\boldsymbol{x}^*\right)}{\partial \boldsymbol{x}^*_d} C_{Y_t}^{-1} \frac{\partial B(\boldsymbol{x}^*)^T}{\partial \boldsymbol{x}^*_e}$$

$$- 2 \frac{\partial^2 B\left(\boldsymbol{x}^*\right)}{\partial \boldsymbol{x}^*_d \partial \boldsymbol{x}^*_e} C_{Y_t}^{-1} B(\boldsymbol{x}^*)^T + \frac{\partial^2 \Phi\left(\boldsymbol{x}^*\right)}{\partial \boldsymbol{x}^*_d \partial \boldsymbol{x}^*_e} \tag{13}$$

Here, the subscribtion d, e represent the dth and eth elements of the input vector. For the square exponential covariance function Φ in (3), the first order and second order partial derivatives of B can be written in the following form shown in (14) and (15).

$$\left.\frac{\partial B^i\left(\boldsymbol{x}^*\right)}{\partial \boldsymbol{x}^*_d}\right|_{\boldsymbol{x}^*=\mu_{\boldsymbol{x}^*}} = \omega_d\left(\boldsymbol{x}^i_d - \mu_{\boldsymbol{x}^*_d}\right) B^i\left(\mu_{\boldsymbol{x}^*}\right) \tag{14}$$

$$\left.\frac{\partial^2 B^i\left(\boldsymbol{x}^*\right)}{\partial \boldsymbol{x}^*_d \partial \boldsymbol{x}^*_e}\right|_{\boldsymbol{x}^*=\mu_{\boldsymbol{x}^*}} = \omega_d[-\delta_{de} + \left(\boldsymbol{x}^i_d \right.$$

$$\left. -\mu_{\boldsymbol{x}^*_d}\right) \omega_e \left(\boldsymbol{x}^i_e - \mu_{\boldsymbol{x}^*_e}\right)] B^i\left(\mu_{\boldsymbol{x}^*}\right) \tag{15}$$

where B^i refers to the ith element in B, and $\frac{\partial^2 \Phi\left(\boldsymbol{x}^*\right)}{\partial \boldsymbol{x}^*_d \partial \boldsymbol{x}^*_e} = 0$.

B. Uncertainty Propagation in Iterative Multi-Step Forecasting

Multi-horizon forecasting can be effectively achieved by employing the multi-step iterative forecasting, where the new estimation $\hat{y}_t$ together with its variance σ_t^2 will be used to construct the new input $\boldsymbol{x}_{t+1}$ and further, to make the next step prediction $\hat{y}_{t+1}$, until the desired steps are achieved. In this procedure, the uncertainty of the new estimation $\hat{y}_{t+j}$ will be passed to the next input $\boldsymbol{x}_{t+j+1}$, and further introduce additional variance to the next estimation $\hat{y}_{t+j+1}$, thus the uncertainty is propagated and continuously accumulated.

At the 1st step, $\boldsymbol{x}_t \sim N(\mu_{\boldsymbol{x}_t}, \Sigma_{\boldsymbol{x}_t})$

$$\boldsymbol{x}_t \sim N\left(\begin{bmatrix} y_t \\ \vdots \\ y_{t+1-L} \end{bmatrix}, \begin{bmatrix} 0 & \cdots & 0 \\ \vdots & \ddots & \vdots \\ 0 & \cdots & 0 \end{bmatrix}\right) \tag{16}$$

Applying TLGP it follows that $\hat{y}_t \sim N(m(\boldsymbol{x}_t), v(\boldsymbol{x}_t) + v_0)$, where $m(\boldsymbol{x}_t)$ equals the mean prediction in (4) and $v(\boldsymbol{x}_t)$ equals the variance in (5).

At the 2nd step, the input $\boldsymbol{x}_{t+1} \sim N(\mu_{\boldsymbol{x}_{t+1}}, \Sigma_{\boldsymbol{x}_{t+1}})$ with randomness is

$$\boldsymbol{x}_{t+1} \sim N\left(\begin{bmatrix} m\left(\boldsymbol{x}_t\right) \\ \vdots \\ y_{t+2-L} \end{bmatrix}, \begin{bmatrix} v\left(\boldsymbol{x}_t\right)+v_0 & \cdots & 0 \\ \vdots & \ddots & \vdots \\ 0 & \cdots & 0 \end{bmatrix}\right) \tag{17}$$

It can be obtained that $\hat{y}_{t+1} \sim N(m(\boldsymbol{x}_{t+1}), v(\boldsymbol{x}_{t+1}) + v_0)$, where $m(\boldsymbol{x}_{t+1})$ still equals the mean in (4) considering the Taylor expansion [23]. However, the uncertainty $v(\boldsymbol{x}_{t+1})$ is made of the variance under the determistic input in (5) and an extra part is determined by the covariance matrix $\Sigma_{\boldsymbol{x}_{t+1}}$ of input $\boldsymbol{x}_{t+1}$ as shown in the Appendix.

At the $k+1$ step, $\boldsymbol{x}_{t+k} \sim N(\mu_{\boldsymbol{x}_{t+k}}, \Sigma_{\boldsymbol{x}_{t+k}})$ in detail as follows

$$N\left(\begin{bmatrix} m\left(\boldsymbol{x}_{t+k-1}\right) \\ \vdots \\ m\left(\boldsymbol{x}_{t+k-L}\right) \end{bmatrix}, \right.$$

$$\left. \times \begin{bmatrix} v\left(\boldsymbol{x}_{t+k-1}\right)+v_0 & \cdots & \mathrm{cov}_{1L} \\ \vdots & \ddots & \vdots \\ \mathrm{cov}_{L1} & \cdots & v\left(\boldsymbol{x}_{t+k-L}\right)+v_0 \end{bmatrix}\right) \tag{18}$$

where cov_{ij} is the cross-covariance

$$\mathrm{cov}_{ij} = \mathrm{cov}\left(y_{t+k-i}, y_{t+k-j}\right) \tag{19}$$

Therefore, it follows that $\hat{y}_{t+k} \sim N(m(\boldsymbol{x}_{t+k}), v(\boldsymbol{x}_{t+k}) + v_0)$, similar to the distribution calculation of $\hat{y}_{t+1}$.

Therefore, it can be concluded that to get $v(\boldsymbol{x}_{t+j})$, $\Sigma_{\boldsymbol{x}_{t+j}}$ must be updated at every step. The covariance matrix of next step prediction $\Sigma_{\boldsymbol{x}_{t+j+1}}$ can be obtained based on $\Sigma_{\boldsymbol{x}_{t+j}}$. First, by removing the last column and the last row of $\Sigma_{\boldsymbol{x}_{t+j}}$, $\Sigma'_{\boldsymbol{x}_{t+j}}$ results. Second, the new cross-covariance terms that appear in the first column of $\Sigma_{\boldsymbol{x}_{t+j+1}}$ can be obtained by constricting $\mathrm{cov}(y_{t+j}, \boldsymbol{x}_{t+j})$ as (20):

$$R = \mathrm{cov}\left(y_{t+j}, \boldsymbol{x}_{t+j}\right) = \left.\frac{\partial \mu\left(\boldsymbol{x}_{t+j}\right)}{\partial \boldsymbol{x}_{t+j}}\right|_{\boldsymbol{x}_{t+i}=\mu_{\boldsymbol{x}_{t+j}}} \Sigma_{\boldsymbol{x}_{t+j}} \tag{20}$$

Thus, resulting in the variance matrix for $\boldsymbol{x}_{t+j+1}$ shown in (19), where R' is obtained by removing the last element of R.

$$\Sigma_{\boldsymbol{x}_{t+j+1}} = \begin{bmatrix} v\left(\boldsymbol{x}_{t+j}\right)+v_0 & R'^{\mathrm{T}} \\ R' & \Sigma'_{\boldsymbol{x}_{t+j}} \end{bmatrix}. \tag{21}$$

With the new variance $v(\boldsymbol{x}_{t+k})$ calculated, the new prediction will give the three interval forecasts directly based on the Gaussian distribution assumption. The uncertainty propagation
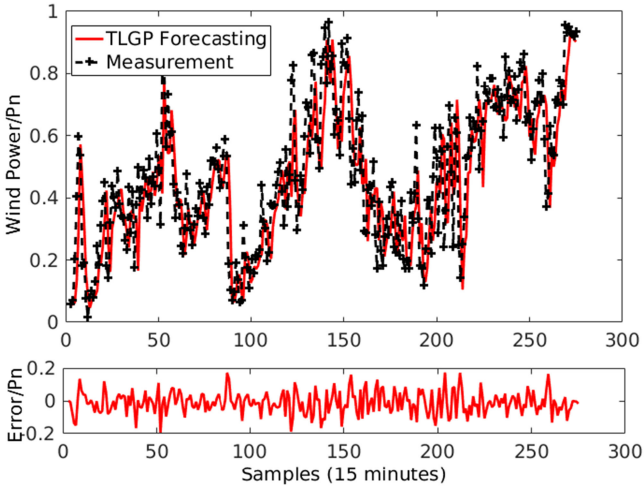
Fig. 1. One step ahead prediction with TLGP in wind farm 'A' [23].

TABLE I
THE OPTIMAL MODEL PARAMETERS FOR TLGP IN WIND FARM 'A'

(L, M)	(6, 8)	**(8, 4)**	(10, 15)	(15, 15)
One step MAE	0.0297	**0.0295**	0.0295	0. 0295
One step RMSE	0.0369	0. **0367**	0. 0367	0.0367
(L, M)	(6, 6)	**(8, 6)**	(10, 8)	(15, 10)
Multi-step MAE	0.0555	0. **0555**	0.0562	0.0591
Multi-step RMSE	0.0676	**0.0674**	0.0681	0.0713

TABLE II
THE IMPROVEMENT OF TLGP OVER BENCHMARK MODELS IN WIND FARM 'A'

Metrics Improvement	max RMSE	mean RMSE	max MAE	mean MAE
Persistence	15.7%	12.8%	18.0%	12.9%
GP	9.13%	6.2%	11.9%	8.72%

for iterative multi-step forecasting can be outlined as follows:

Step 1: For one-step ahead predictions, a zero matrix of covariance is initialized. The mean and variance of $\hat{y}_t$ are estimated by TLGP with deterministic inputs as in (4) and (5).

Step 2: For the jth ($k > j > 0$) step ahead prediction, the previous output $\hat{y}_{t+j}$ is used to construct the new input vector $\boldsymbol{x}_{t+j+1}$ and further predict the mean value of $\hat{y}_{t+j+1}$ using TLGP as defined in (4).

Step 3: Estimate R with (20). Remove the last element of R and add up the variance $v(\boldsymbol{x}_{t+j}) + v_0$ of $\hat{y}_{t+j}$, leading to the construction of a new variance $\Sigma_{\boldsymbol{x}_{t+j+1}}$ of $\boldsymbol{x}_{t+j+1}$ as shown in (21).

Step 4: Estimate the new variance $v_{tl}(\boldsymbol{x}_{t+j+1}) + v_0$ of $\hat{y}_{t+j+1}$ with (11) where $\Sigma_{\boldsymbol{x}^*} = \Sigma_{\boldsymbol{x}_{t+j+1}}$. Thus, the mean and variance of $\hat{y}_{t+j+1}$ can be used for the next step prediction.

Step 5: Decide whether the desired horizon has been reached. If not go to Step 2, otherwise terminate.

IV. CASE STUDIES AND RESULT ANALYSIS

A. Wind Farm 'A' in Ireland

Power generation data from a wind farm in Donegal in North West Ireland is used to analyze the uncertainty propagation in wind power forecasting with TLGP. The influence of the North Atlantic sea wind and lake-hill breeze at this wind farm makes wind power generation more unpredictable and thus more convincing for any conclusion drawn from the study. The deterministic forecasting of this wind farm and the parameter optimization procedure has been addressed in [29]. Wind generation data of one year were collected up to June 2004, averaged with a time resolution of 15 minutes, and then normalized by the full capacity to predict the output of the first 3 days in July 2004 as in Fig. 1. In [29], the data used was in unit of MWHr representing the overall wind energy output in a quarter of hour, thus the wind generation in [29] has similar shape with Fig. 1 of this paper, but shows a fixed ratio of 0.25. Based on the existing

point forecasting results from [29], this work investigates the uncertainty propagation of iterative multi-step forecasting and determines the interval forecasting results.

1) Model Training and Mean Value Forecasting: The squared exponential covariance function is still used in TLGP for wind power forecasting. The trial-and-error method is used to identify the optimal parameters (L, M) in TLGP. However, in this work further tests were carried under different (L, M) settings and the best results are given in Table I. The optimal model with the least multi-step errors is (8, 6) which also shows a satisfactory one-step ahead forecasting performance. Such findings agree with the experiment settings in [29]. The input vector is required to include measurements from 2 hours ahead to implement TLGP.

In [23], the deterministic forecasting results of TLGP were plotted to compare the forecasting performance with other benchmark models. The forecasting metrics were evaluated with root mean square error (RMSE) and mean absolute error (MAE). Metric comparison has shown the effectiveness of TLGP for point forecasting. In order to better show the interval forecasting results, in this work the result of point forecasting is plotted again in Fig. 1 as in [29]. Further analysis shows that the maximum normalized error could reach 0.33 while the average is 0.11. Table II shows that TLGP made over 6% and 12% improvement over the deterministic forecasting results of the GP and persistence model separately. The uncertainty involved in this mean value prediction will be discussed in the next section. The benchmark models such as persistence, ARMA [30] and neural network will be referenced based on which the empirical error will be investigated and interval forecasts will be implemented.

2) Analytical Interval Forecasts With TLGP: Fig. 2 shows the three predictive intervals for one-step ahead prediction. Region 1 represents prediction interval I with nominal confidence probability of 68%. Region 1 and 2 together refer to prediction interval II of 95% and Region 1, 2 and 3 together represent prediction interval III with nominal confidence probability of 99.7%, as illustrated in Section II. In most cases, the real outputs represented by the dashed red line stay within Region I, which is the darkest region in the center. However, some predictions leave Region I and enter Region II or even
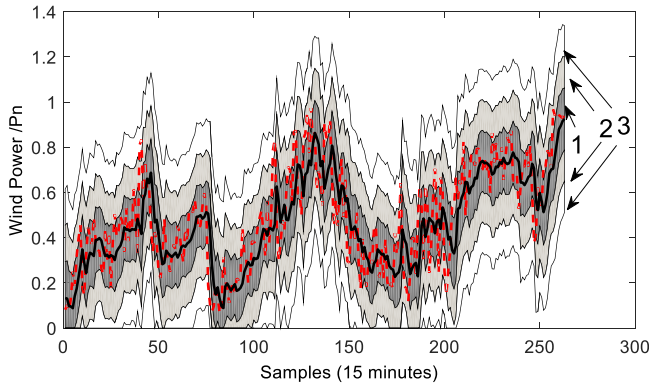
Fig. 2. The one-step probabilistic forecasting results of 'A' by TLGP. The red dashed line represents the real measurements while the shaded area represents the predicted intervals with different confidence.
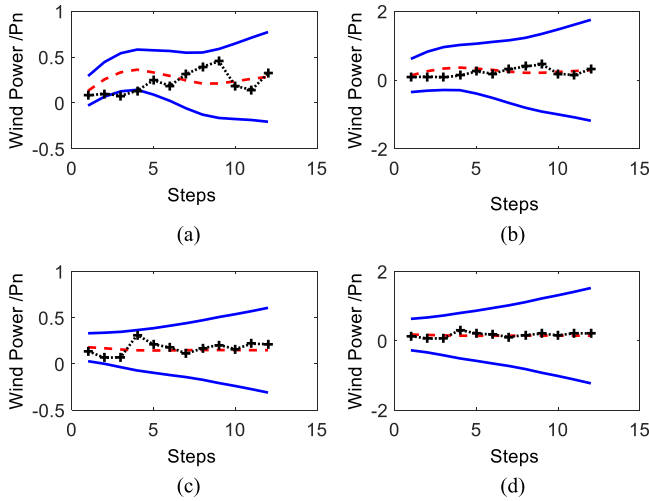

Fig. 3. The uncertainty propagation of 'A' at the 1st sample and the 81st sample. The solid lines represent the bounds of confident regions, the dashed line without marker shows the multi-step prediction and the dashed line with marker shows the real measurement.

Region III. This gives an intuitive indication of the three prediction intervals with different coverage rate.

3) Uncertainty Propagation for Multi-Step Forecasting: Prediction uncertainty propagates and accumulates in iterative multi-step ahead prediction. The uncertainty, represented by std (standard deviation), increases in multi-step ahead predictions which is clearly shown in Fig. 3. While (a) and (b) show the $\mu \pm \sigma$ and $\mu \pm 3\sigma$ bounds of the 12 step predictions based on the 1st time instants respectively, (c) and (d) show those of the 81st time instants. The bounds are enlarged as the number of steps increases. Besides, the $\mu \pm 3\sigma$ interval (Interval III) in (b) and (d) cover broader area than (a) and (c) (Interval I). Further, as shown in (a), the 3rd real measurement leaves Interval I, but stays within the Interval III of (b), showing less reliability in the interval forecasting of this point. However, in (c) and (d) all the predictions stay within both bounds of Interval I and Interval III, showing the reliability of predictions at the 81st time instants.

Fig. 4 shows the comparison of the multi-step prediction uncertainty at different time instants based on the derived
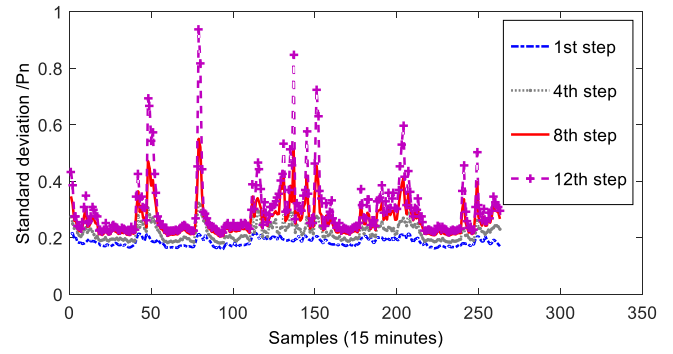

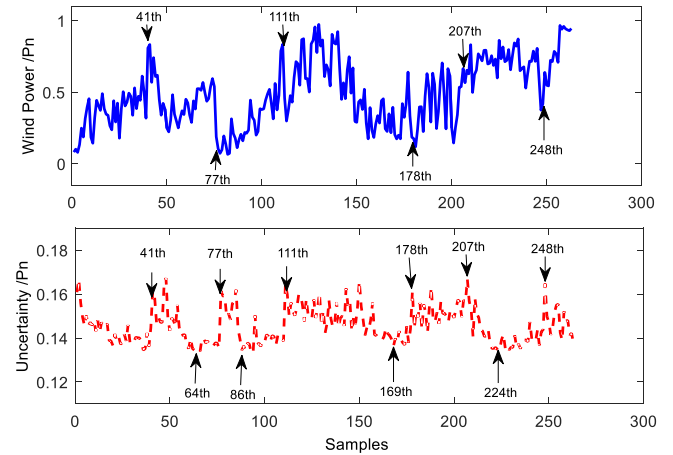Fig. 4. The uncertainty of Interval I for the testing points at varied steps with TLGP of wind farm 'A.'

Fig. 5. Real measurement (top) and the corresponding one-step uncertainty of forecasting with TLGP (bottom) of wind farm 'A.'

uncertainty propagation rule presented earlier. The uncertainty distributions of the one-step ahead predictions are relatively stable and only exhibit small variations at different points. However, for multi-step ahead predictions (such as 12th steps ahead), the uncertainty begins to undulate severely and such uncertainties escalate with the number of prediction steps. This uncertainty information can be used to estimate other quantiles of new predictions and can help to develop better plans for economic dispatch and unit commitment of wind power.

4) Uncertainty Analysis at Different Prediction Points: Fig. 5 shows the standard deviation and the real measurements for one-step ahead predictions. It shows that the uncertainty/std is less than 0.04, e.g., less than 4% of the power capacity. This is a very close fit with the real measurements. Every prediction point shows similar uncertainty. It can also be seen that with the changes between every two consecutive points, the uncertainty grows rapidly during ramping events. For example, the uncertainty increases dramatically at the 41th, the 111th and the 207th samples, due to the rapid increase in wind power generation just before these time instants. Further, other obvious large increases in uncertainty occur at the 77th, the 178th, and the 248th points, which are caused by a sudden drop of wind power generation before those time instants. Less uncertainty is observed when the wind power generation is relatively stable.
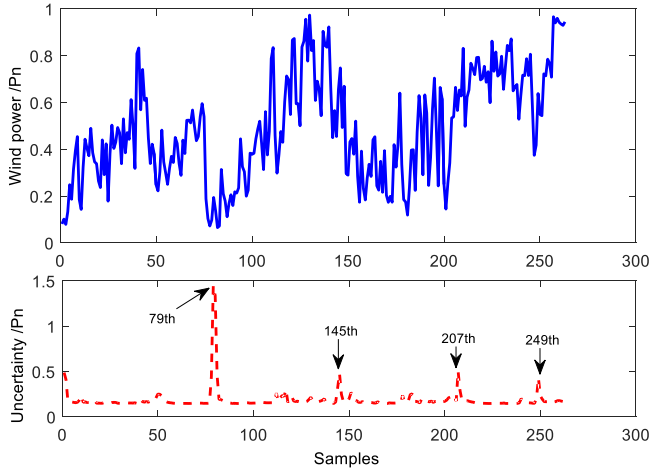
Fig. 6. Real measurement (top) and the corresponding 12-step uncertainty of forecasting with TLGP (bottom) of wind farm 'A.'
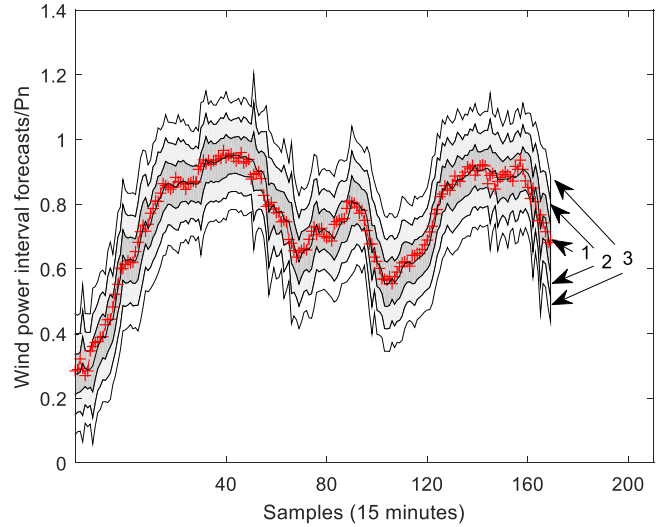

Fig. 7. The three-step interval forecasting results of Ireland by TLGP. The marked read line represents the real measurements, and the other shaded area represents intervals with different confidence with the middle line representing the mean of probabilistic forecasting.
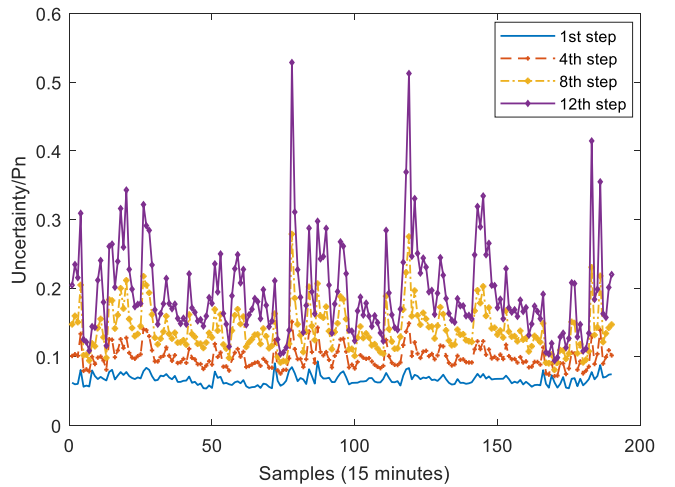

Fig. 8. The uncertainty of Interval I for the testing points at varied steps with TLGP for wind power of Ireland.

For twelve-step ahead predictions, the uncertainty is shown in Fig. 6. It shows a few significant peak values including some points developed from the one-step ahead uncertainty peak points in Fig. 5. For example, the 79th, the 207th and the 249th points in Fig. 6 are developed from the 77th, the 207th, and the 248th points in Fig. 5. It is interesting that these uncertainty peak points are shifted as in the multi-step ahead predictions. Thus, it appears that uncertainties accumulate and shift forward along the iterative multi-step forecasting horizon. Some of the one-step peak uncertainties are averaged out in the twelve-step ahead predictions, such as the 41th, 111th, and 178th points. On the other hand, at some points, the uncertainty accumulates very fast to generate some small peaks in the 12th step ahead predictions, such as the 145th point in Fig. 6.

B. Overall Generation of Ireland

Regional wind power forecasting is important in terms of wind penetrating, energy scheduling and power grid stabilizing within large inter or intra areas. The accurate forecasting of regional wind power will benefit the cooperation between different regions for grid balancing, wind integration, security of energy supply. Time series forecasting show its unique advantage regarding the dispersed wind distribution across the region while NWP becomes out of effect for forecasting power as a whole. In [23], the authors looked at the accuracy of using TLGP for whole Ireland wind power forecasting. In this paper, the interval forecasts will be further developed with (L, M) remaining the same as (10, 14) to minimize the average error of multi-step forecasting.

The interval forecasting results for the wind power of Ireland are shown in Fig. 7. Similar to wind farm 'A', it has three probabilistic intervals corresponding to 3 different confidence levels, but show more confident (condense) interval estimation results.

Fig. 8 shows half of the width of interval I at different time instants and various prediction steps for Ireland. It shows that the peak values happen at about the same time instants for different time horizons and a small bump for one step forecasting may get accumulated and become a significant peak for multi-step forecasting. This is similar to the pattern interval forecast for wind farm 'A'.

The uncertainty distribution over the investigated period for the whole Ireland wind power forecasting show similar trends with that of wind farm 'A', only with more confident and condense interval forecasts due to the smooth change of generation. The interval forecast results in this section showed the capability of proposed network in approximating uncertainty propagation for iterative multi-step forecasting. In the following sections, the interval forecast results will be further analysed and compared with other benchmark models. If the conclusions stand for this small wind farm, then it will be also effective for the whole island.
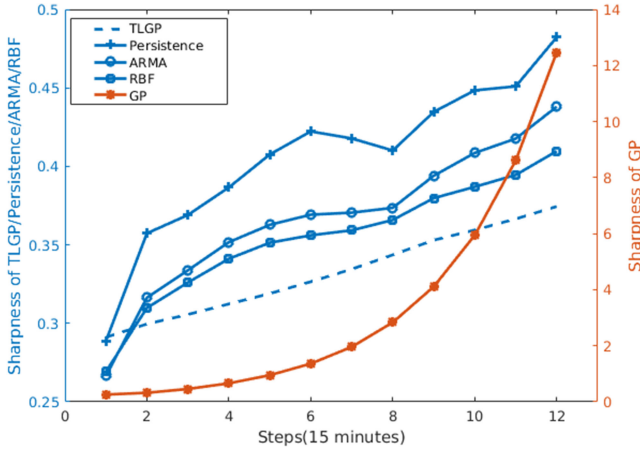
Fig. 9. The sharpness diagram with respect to the horizons for wind farm 'A.'

V. PROBABILISTIC EVALUATION AND DISCUSSIONS

A. Wind Farm 'A' in Ireland

1) Sharpness/Uncertainty Evaluation and Comparison: As one the of evaluation metrics of probabilistic forecasting, the sharpness refers to the mean size of the interval in interval forecasts [13]. The size of each interval in this work is proportional to the std with a coefficient c of 2, 4 and 6 respectively in (22) where k refers to the prediction steps. As Interval II and III have a very high coverage rate of 95% and 99.7%, which accounts for the extreme error and outliers in the prediction, we will take Interval I and compare the sharpness of different methods. The sharpness of the other two intervals will be proportional to that of Interval I. The sharpness comparison of Interval I with respect to the multi-steps is shown in Fig. 9.

$$\bar{\delta}_k = \frac{1}{N} \sum_{t=1}^{N} c\sigma_{t+k|t} \qquad (22)$$

In [18], several benchmark forecasting models have been assessed, including the persistence model, ARMA and the neural network model. In [15], the authors provided a parametric framework of analyzing the empirical errors of these deterministic forecasting methods and employing the uncertainty of error for interval forecasts. The forecasting error of these benchmark models were analyzed and the parametric interval forecasts were implemented with the standard deviation representing the uncertainty. The probabilistic forecasting results of these benchmark models are compared with those of GP and TLGP. As the five models show significantly different prediction ranges, two y-axes are used. The right represents the performance of GP, and the left is for the other models as shown in Fig. 9. The sharpness of persistence model, ARMA and neural network models are far better than GP for the iterative multistep forecasting and even comparable to TLGP for the first step prediction. However, these models are inferior to TLGP for multi-step interval forecasts as the error accumulates. As these methods only generate overall empirical uncertainty estimation over the time space, no prediction interval can be estimated for each individual time instance.
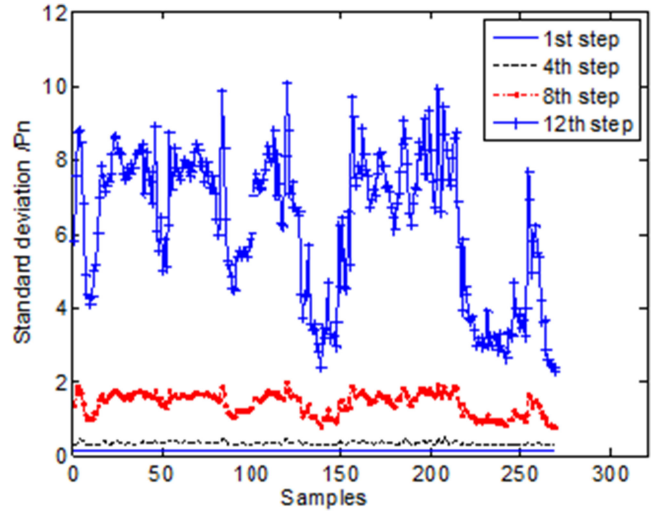

Fig. 10. The standard deviation distribution of forecasting at varied steps with GP for wind farm 'A.'
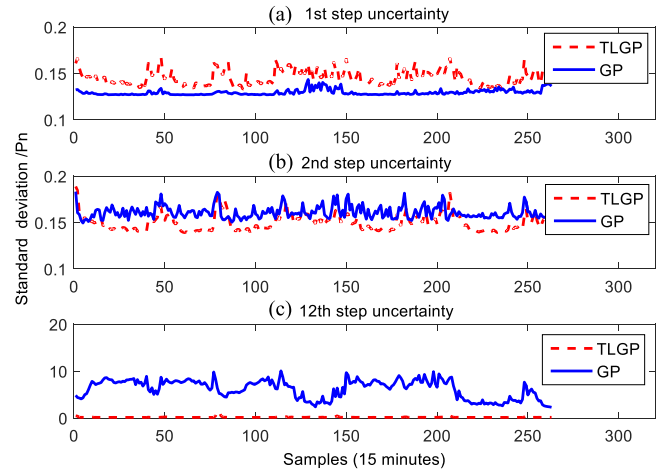

Fig. 11. The standard deviation comparison of TLGP and GP at varied steps for wind farm 'A.'

A better look at the interval forecast of GP and its comparison with TLGP is shown in Figs. 10 and 11 respectively. The variance of noise v_0 has a significant impact on the uncertainty accumulation rate. In the uncertainty analysis, the optimized v_0 in both TLGP and GP are approximately the same. The uncertainty propagates very fast in multi-step ahead predictions for GP. For the one-step predictions in Fig. 11(a), TLGP shows higher prediction uncertainty than GP almost at every testing point. This is because TLGP employs less data in each moving window for prediction, thus produce results with less confidence. However, for multi-step ahead forecasting, TLGP starts to outperform GP with smaller uncertainty from the 2nd step as shown in (b). Furthermore, for the twelve-step ahead prediction, the advantages of TLGP become more obvious, for example the mean uncertainty of GP is approximately 7, while it is only 0.18 for TLGP. This analysis confirms that uncertainty accumulates much more slowly for TLGP.

2) The Reliability Evaluation and Comparison: Since the intervals have been defined in terms of the std of each

TABLE III
THE EMPIRICAL PROBABILITIES OF DIFFERENT INTERVALS AND THE AVERAGE
OF PREDICTED STD OF TLGP FOR WIND FARM 'A'

Prediction steps	1	2	3	4	5	6
Averaged std	0.1456	0.1498	0.1528	0.1562	0.1595	0.1633
Interval I	68.8%	64.3%	64.6%	64.3%	64.3%	63.9%
Interval II	95.4%	93.5%	93.5%	92.4%	91.3%	90.8%
Interval III	100%	100%	99.6%	99.6%	100%	100%
Prediction steps	7	8	9	10	11	12
Averaged std	0.1673	0.1718	0.1765	0.1797	0.1833	0.1872
Interval I	65.0%	60.5%	59.3%	55.9%	55.5%	50.9%
Interval II	90.5%	89.7%	88.6%	87.1%	86.3%	85.9%
Interval III	99.6%	99.6%	98.5%	98.9%	98.9%	98.9%

TABLE IV
THE EMPIRICAL PROBABILITIES OF DIFFERENT INTERVALS AND THE AVERAGE
OF PREDICTED STD OF GP FOR WIND FARM 'A'

Prediction steps	1	2	3	4	5	6
Averaged std	0.1295	0.1609	0.2293	0.3304	0.4750	0.6809
Interval I	68.4%	71.8%	84.8%	94.42%	99.63%	100%
Interval II	94.8%	95.2%	99.3%	100%	100%	100%
Interval III	99.6%	100%	100%	100%	100%	100%
Prediction steps	7	8	9	10	11	12
Averaged std	0.9805	1.4172	2.0548	2.9713	4.3041	6.2327
Interval I	100%	100%	100%	100%	100%	100%
Interval II	100%	100%	100%	100%	100%	100%
Interval III	100%	100%	100%	100%	100%	100%

Fig. 12. The reliability comparison of TLGP with other benchmark models for wind farm 'A.'

prediction (for one-step or multi-step), the interval is varying at different time instants and horizons. The probability of the real wind power generation falling in each interval can be obtained. For a good prediction, the empirical (i.e., observed) probability and the defined coverage rate (i.e., nominal probability) should be as close as possible. This property is referred to as reliability. Moreover, bias or deviation, b_k has been defined as the difference between the nominal probabilities α and the empirical probabilities α_k as an evaluation metric for reliability [13].

$$b_k = \alpha - \alpha_k \tag{23}$$

Empirical probabilities and estimated uncertainty (i.e., std) at each horizon for TLGP forecasting are shown in Table III. For longer prediction horizons, the empirical probabilities tend to decrease slowly. This is because for TLGP, the uncertainty (std) does not accumulate as fast as prediction error as the mean value propagates. The average empirical probability over different forecasting steps ahead are 61.4%, 90.5%, and 99.5% in Interval I, II and III, respectively for TLGP.

Empirical probabilities and estimated uncertainty (standard deviation) at each horizon for GP are shown in Table IV. Conversely, the probabilities in each region tend to increase as the forecasting horizon increases and stabilize finally at 100%. This is because for GP the uncertainty (i.e., std) accumulates very fast so although the forecasting error has enlarged, the probability of the wind power generation falling in the interval is still
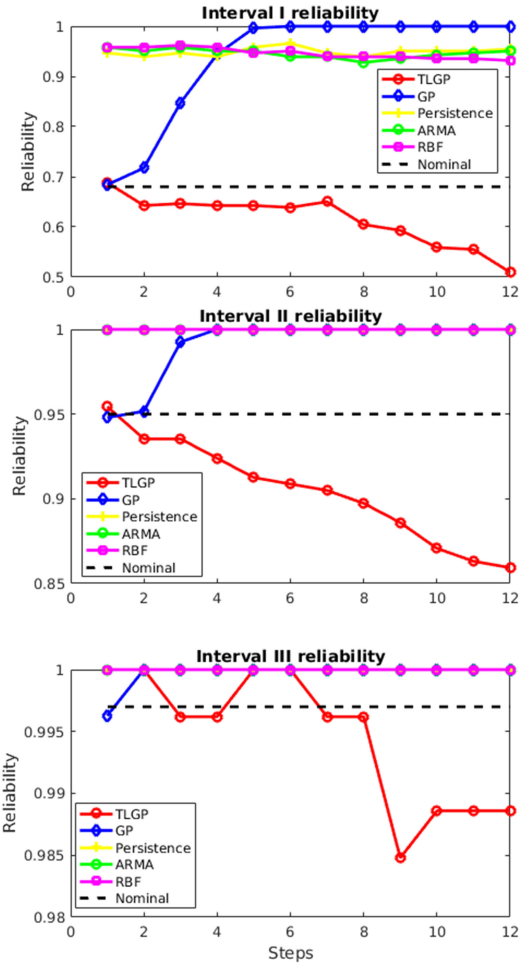
increased. The average probabilities with respect to different step forecasting in every region are 93.2%, 99.1% and 99.97% in Interval I, II and III, respectively for GP.

The above observations are further illustrated in Fig. 12. The empirical probability results for TLGP tend to decrease with multi-steps, whereas for GP they tend to increase and for other benchmark models, they tend to stay the same. Furthermore, the uncertainty accumulation for all the benchmark models are very fast and the confidence probability approaches 100% very quickly. The large empirical uncertainty for GP is caused by the significant predicted variance at each point as shown in Fig. 9. The black dashed line represents the ideal coverage probability for 'perfect' probabilistic forecasting. It shows in the Interval I, interval forecasting with TLGP shows much better reliability than with GP or any other reference models. While the refence models usually show bigger coverage rate than the nominal, TLGP is displaying a smaller one indicating a slow uncertainty accumulation over the iterative multi-steps. By calculating the overall mean absolute bias and mean empirical probability, Table V shows that the reliability of TLGP outperforms that of GP and other models greatly in Interval I and performs about the same in Interval II & III. This indicates that the estimated uncertainty of the probabilistic forecasting for TLGP fits the data
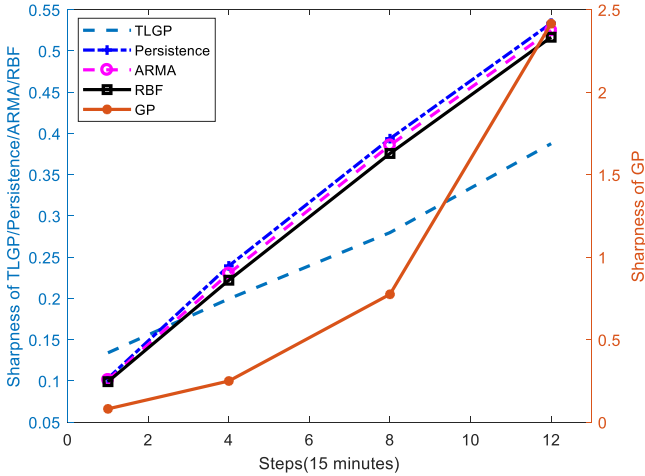
Fig. 13. The sharpness diagram with respect to the forecasting horizons for wind generation of Ireland.

TABLE V
THE MEAN EMPIRICAL PROBABILITY AND RELIABILITY BIAS AT THREE INTERVALS WITH DIFFERENT METHODS FOR WIND FARM 'A'

Methods		Interval I	Interval II	Interval III
Empirical probability	TLGP	61.4%	90.5%	99.5%
	GP	93.2%	99.1%	99.97%
	Persistence	94.9%	100%	100%
	ARMA	94.6%	100%	100%
	RBF	94.6%	100%	100%
	Nominal	68%	95%	99.7%
Reliability bias	TLGP	6.6%	4.5%	0.2%
	GP	25.2%	-4.1%	-0.3%
	Persistence	-26.9%	-5%	-0.3%
	ARMA	-26.6%	-5%	-0.3%
	RBF	-26.6%	-5%	-0.3%

better. This is another advantage of TLGP. It is worth noticing that the three benchmark models have quite similar reliability although their sharpness as shown in Fig. 11 is apparently different. This is probably due to two reasons. Firstly, as shown in Table V is the averaged reliability over 12 forecasting horizons. It is apparent that the minor difference of their reliability trends, as reflected in the first figure of Fig. 12, is filtered out while averaging the reliability scores. Secondly, the distribution of the errors tends to be too long-tailed, so when the standard deviation is used to evaluate the mean reliability, the interval forecasting becomes over-confident with 100% reliability. This reveals the difficulty of parametric interval forecasts.

B. Overall Generation of Ireland

1) Sharpness/Uncertainty Evaluation and Comparison: To evaluate the sharpness of interval forecast for the overall wind generation of Ireland, the same method was implemented for Interval I and compared with the other benchmark models as in part A. GP again shows quick uncertainty accumulation but the trend slows down in comparison with that of wind farm 'A'. The sharpness of TLGP shows slowest accumulation with iterative
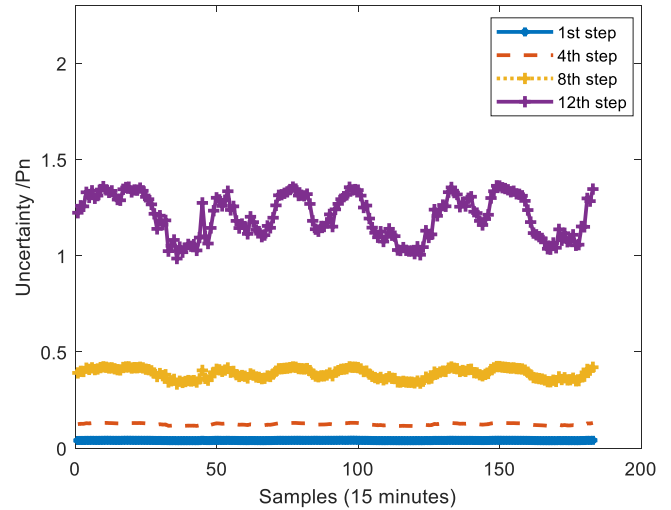

Fig. 14. The standard deviation distribution of forecasting at varied steps with GP for wind generation of Ireland.
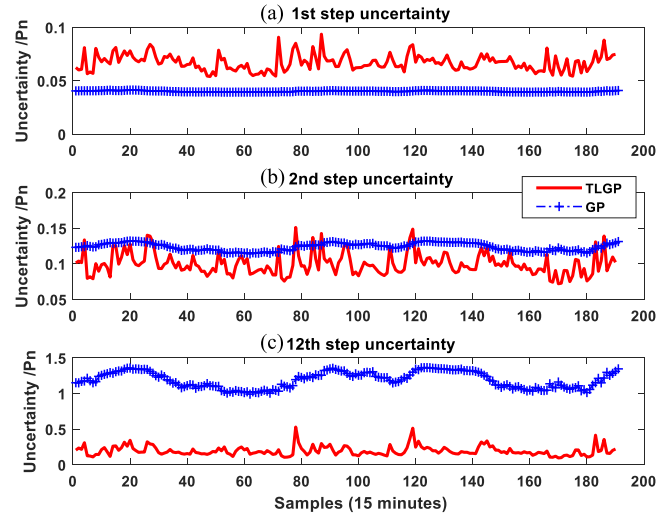

Fig. 15. The standard deviation comparison of TLGP and GP at varied steps for wind generation of Ireland.

multi-step forecasting and generates sharpest interval forecasts. Similar to part A, we will further illustrate the detailed interval forecasts at various time instants for multi-horizons with GP and the comparison with that of TLGP in Figs. 14 and 15. Although TLGP shows more uncertainty for one step forecasting due to the limited data used, but the uncertainty accumulates is the slowest among the five models used for iterative multi-step forecasting. The sharpness comparison show very similar results with that of wind farm 'A'.

2) The Reliability Evaluation and Comparison: The reliability of different interval forecast methods are evaluated and compared in this part. Similar to the results for wind farm 'A', the reliability of TLGP shows most Gaussian-like behavior, which verifies the assumption of local Gaussian Processes in each time window. The reliability trend of different methods are shown in Fig. 16 and the reliability bias for three predicted intervals is listed in Table VI. It is worth noting the interval forecasts with
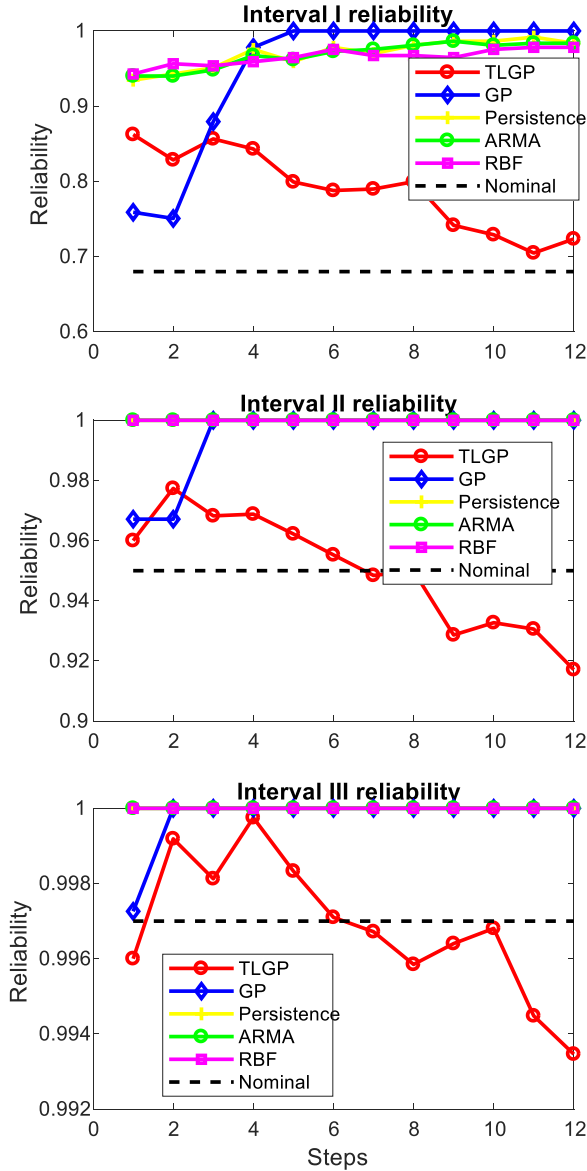
Fig. 16. The reliability comparison of TLGP with other benchmark models for wind generation of Ireland at three predicted intervals.

TABLE VI
THE RELIABILITY BIAS AT THREE INTERVALS WITH DIFFERENT METHODS FOR WIND GENERATION OF IRELAND

Methods		Interval I	Interval II	Interval III
	TLGP	-6%	0.06%	0.01%
	GP	-26.7%	-4.5%	-0.3%
Reliability bias	Persistence	-29%	-5%	-0.3%
	ARMA	-28.8%	-5%	-0.3%
	RBF	-28.5%	-5%	-0.3%

TLGP show better qualities, e.g., sharpness and reliability bias for the wind generation of whole Ireland in comparison with that of a small wind farm 'A' due to the smooth change of wind generation in a large region.

VI. CONCLUSION

Both TLGP and GP are convenient for interval forecasting by nature with no need to calculate each of the single quantile numerically. For the non-Gaussian noise in the wind generation which is generated by the non-linear transformation between wind speed and wind power, TLGP was proposed to approximate Gaussian-like behavior in each short time window. In this work, the uncertainty propagation of the iterative multistep forecasting was analyzed for the first time and the analytical interval forecasts were given for each step. While the traditional probabilistic approach relies mainly on statistically analyzing the forecasting error, this method provide one way of looking at the uncertainty variation at different time instants for different forecasting horizons. The probabilistic forecasting results were evaluated after TLGP and GP were applied to short-term wind power forecasting in a wind farm in Ireland and for the whole Ireland. Three main conclusions can be drawn from this work. First, TLGP shows more accurate and more confident interval forecast for smoother and more steadily changing wind generation with an exception for ramp events forecasting. Uncertainties show up mainly and accumulate significantly at the ramping points, and they shift forward as the forecasting horizon expands iteratively. Secondly, for one-step forecasting, TLGP shows higher prediction uncertainty because a limited number of data are used, but the uncertainties accumulate much more slowly for iterative multi-step forecasting. It generates higher reliability over the named three intervals and better sharpness on the shape of distribution, which makes the probabilistic forecasting with TLGP more trustworthy. More importantly, the reliability of proposed method approaches that of standard Gaussian distribution which proves the assumption that TLGP is more Gaussian-like. Such analytical method of analyzing the uncertainty propagation for the iterative multi-step wind power forecasting has not been proposed before. Hopefully, it will stimulate research for other methods under investigation.

APPENDIX

A. The Mean Value Estimation Under a Random Input

With the law of iterated expectations, the new mean output is the expectation of the old mean function.

$$m\left(\boldsymbol{x}^*\right) = E_{\boldsymbol{x}^*}\left[\mu\left(\boldsymbol{x}^*\right)\right] \qquad (24)$$

The first order Taylor expansion can be written as follows,

$$\mu\left(\boldsymbol{x}^*\right) = \mu\left(\mu_{\boldsymbol{x}^*}\right) + \left.\frac{\partial \mu\left(\boldsymbol{x}^*\right)}{\partial \boldsymbol{x}^*}\right|_{\boldsymbol{x}^*=\mu_{\boldsymbol{x}^*}}^{\mathrm{T}}$$
$$\times \left(\boldsymbol{x}^* - \mu_{\boldsymbol{x}^*}\right) + O\left(\left\|\boldsymbol{x}^* - \mu_{\boldsymbol{x}^*}\right\|^2\right) \qquad (25)$$

If its first order differentiation is finite around x^*, thus we have $m(\boldsymbol{x}^*) = \mu(\mu_{\boldsymbol{x}^*})$ in (10) which means the new mean stays the same with the forecasting result under deterministic input.

B. The Variance Estimation Under a Random Input

With the law of conditional variance, the new variance of output will follow

$$v\left(\boldsymbol{x}^*\right) = E_{\boldsymbol{x}^*}\left(\sigma^2\left(\boldsymbol{x}^*\right)\right) + Var_{\boldsymbol{x}^*}\left(\mu\left(\boldsymbol{x}^*\right)\right) \qquad (26)$$

Expanding the first term with Taylor Series in second order gives

$$\sigma^2\left(\boldsymbol{x}^*\right) = \sigma^2\left(\mu_{\boldsymbol{x}^*}\right) + \left.\frac{\partial\sigma^2\left(\boldsymbol{x}^*\right)}{\partial\boldsymbol{x}^*}\right|_{\boldsymbol{x}^*=\mu_{\boldsymbol{x}^*}}^{\mathrm{T}}\left(\boldsymbol{x}^* - \mu_{\boldsymbol{x}^*}\right)$$
$$+ \frac{1}{2}(\boldsymbol{x}^* - \mu_{\boldsymbol{x}^*})^{\mathrm{T}}\left.\frac{\partial^2\sigma^2\left(\boldsymbol{x}^*\right)}{\partial\boldsymbol{x}^*\partial\boldsymbol{x}^{*\mathrm{T}}}\left(\boldsymbol{x}^* - \mu_{\boldsymbol{x}^*}\right)\right|_{\boldsymbol{x}^*=\mu_{\boldsymbol{x}^*}}^{\mathrm{T}}$$
$$+ O\left(\|\boldsymbol{x}^* - \mu_{\boldsymbol{x}^*}\|^3\right) \qquad (27)$$

Thus we have the following expectation

$$E_{\boldsymbol{x}^*}\left(\sigma^2\left(\boldsymbol{x}^*\right)\right) \approx \sigma^2\left(\mu_{\boldsymbol{x}^*}\right) + E_{\boldsymbol{x}^*}$$
$$\times \left(\frac{1}{2}(\boldsymbol{x}^* - \mu_{\boldsymbol{x}^*})^{\mathrm{T}}\frac{\partial^2\sigma^2\left(\boldsymbol{x}^*\right)}{\partial\boldsymbol{x}^*\partial(\boldsymbol{x}^*)^{\mathrm{T}}}\left(\boldsymbol{x}^* - \mu_{\boldsymbol{x}^*}\right)\right)$$
$$= \sigma^2\left(\mu_{\boldsymbol{x}^*}\right) + \frac{1}{2}\mathrm{Tr}\left\{\left.\frac{\partial^2\sigma^2\left(\boldsymbol{x}^*\right)}{\partial\boldsymbol{x}^*\partial\boldsymbol{x}^{*\mathrm{T}}}\right|_{\boldsymbol{x}^*=\mu_{\boldsymbol{x}^*}}\Sigma_{\boldsymbol{x}^*}\right\} \qquad (28)$$

Substitute (25) in the second term of (26), it follows

$$Var_{\boldsymbol{x}^*}\left(\mu\left(\boldsymbol{x}^*\right)\right) \approx Var_{\boldsymbol{x}^*}$$
$$\times \left(\mu\left(\mu_{\boldsymbol{x}^*}\right) + \left.\frac{\partial\mu\left(\boldsymbol{x}^*\right)}{\partial\boldsymbol{x}^*}\right|_{\boldsymbol{x}^*=\mu_{\boldsymbol{x}^*}}^{\mathrm{T}}\left(\boldsymbol{x}^* - \mu_{\boldsymbol{x}^*}\right)\right)$$
$$= \left.\frac{\partial\mu_{\boldsymbol{x}^*}}{\partial\boldsymbol{x}^*}\right|_{\boldsymbol{x}^*=\mu_{\boldsymbol{x}^*}}^{\mathrm{T}}\Sigma_{\boldsymbol{x}^*}\left.\frac{\partial\mu_{\boldsymbol{x}^*}}{\partial\boldsymbol{x}^*}\right|_{\boldsymbol{x}^*=\mu_{\boldsymbol{x}^*}}. \qquad (29)$$

Thus the new variance function in (26) is transformed into (11) which contains an additional term in comparison with the uncertainty result under a deterministic input in (5).

ACKNOWLEDGMENT

REFERENCES

[1] A. M. Foley, A. Marvuglia, P. G. Leahy, and E. J. McKeogh, "A review of current methods and advances in wind power prediction and forecasting," *Renewable Energy*, vol. 7, no. 1, pp. 1–8, 2012.

[2] Y. Zhan, Q. P. Zheng, J. Wang, and P. Pinson, "Decision-dependent stochastic generation expansion planning with large amounts of wind power," *IEEE Trans. Power Syst.*, vol. 32, no. 4, pp. 3015–3026, 2017.

[3] J. Devlin, K. Li, P. Higgins, and A. Foley, "System flexibility provision using short term grid scale storage," *IET Gener. Transmiss. Distrib.*, vol. 10, no. 3, pp. 697–703, 2016.

[4] E. Du *et al.*, "Managing wind power uncertainty through strategic reserve purchasing," *IEEE Trans. Power Syst.*, vol. 32, no. 4, pp. 2547–2559, Jul. 2017.

[5] A. R. W. Bruce, J. Gibbins, G. P. Harrison, and H. Chalmers, "Operational flexibility of future generation portfolios using high spatial- and temporal-resolution wind data," *IEEE Trans. Sustain. Energy*, vol. 7, no. 2, pp. 697–707, Apr. 2016.

[6] A. Botterud *et al.*, "Demand dispatch and probabilistic wind power forecasting in unit commitment and economic dispatch: A case study of Illinois," *IEEE Trans. Sustain. Energy*, vol. 4, no. 1, pp. 250–261, Jan. 2013.

[7] P. Pinson, C. Chevallier, and G. N. Kariniotakis, "Trading wind generation from short-term probabilistic forecasts of wind power," *IEEE Trans. Power Syst.*, vol. 22, no. 3, pp. 1148–1156, Aug. 2007.

[8] J. B. Bremnes, "Probabilistic wind power forecasts using local quantile regression," *Wind Energy*, vol. 7, no. 1, pp. 47–54, 2004.

[9] C. Wan, Z. Xu, P. Pinson, Z. Y. Dong, and K. P. Wong, "Probabilistic forecasting of wind power generation using extreme learning machine," *IEEE Trans. Power Syst.*, vol. 29, no. 3, pp. 1033–1044, May 2014.

[10] J. Dowell and P. Pinson, "Very-short-term probabilistic wind power forecasts by sparse vector autoregression," *IEEE Trans. Smart Grid*, vol. 7, no. 2, pp. 763–770, Mar. 2016.

[11] P. Pinson and G. N. Kariniotakis, "Wind power forecasting using fuzzy neural networks enhanced with on-line prediction risk assessment," in *IEEE Bologna Power Tech Conf.*, Bologna, Italy, 2003, vol. 2, pp. 8–16.

[12] P. Pinson and G. Kariniotakis, "Conditional prediction intervals of wind power generation," *IEEE Trans. Power Syst.*, vol. 25, no. 4, pp. 1845–1856, Nov. 2010.

[13] P. Pinson, H.A. Nielsen, J. K. Møller, H. Madsen, and G. N. Kariniotakis, "Non-parametric probabilistic forecasts of wind power: Required properties and evaluation," *Wind Energy*, vol. 10, no. 6, pp. 497–516, 2007.

[14] Y. Zhang, J. Wang, and X. Wang, "Review on probabilistic forecasting of wind power generation," *Renewable Sustain. Energy Rev.*, vol. 32, pp. 255–270, 2014.

[15] A. P. A. da Silva and L. S. Moulin, "Confidence intervals for neural network based short-term load forecasting," *IEEE Trans. Power Syst.*, vol. 15, no. 4, pp. 1191–1196, Nov. 2000.

[16] C. Wan, Z. Xu, P. Pinson, Z. Y. Dong, and K. P. Wong, "Optimal prediction intervals of wind power generation," *IEEE Trans. Power Syst.*, vol. 29, no. 3, pp. 1166–1174, May 2014.

[17] A. Khosravi, S. Nahavandi, and D. Creighton, "Prediction intervals for short-term wind farm power generation forecasts," *IEEE Trans. Sustain. Energy*, vol. 4, no. 3, pp. 602–610, Jul. 2013.

[18] J. Yan, K. Li, E. Bai, J. Deng, and A. M. Foley, "Hybrid probabilistic wind power forecasting using temporally local Gaussian process," *IEEE Trans. Sustain. Energy*, vol. 7, no. 1, pp. 87–95, Jan. 2016.

[19] A. Lau and P. McSharry, "Approaches for multistep density forecasts with application to aggregated wind power," *Ann. Appl. Statist.*, vol. 4, pp. 1311–1341, 2010.

[20] M. Lange, "On the uncertainty of wind power predictions-Analysis of the forecast accuracy and statistical distribution of errors," *J. Solar Energy Eng.*, vol. 127, no. 2, pp. 177–184, 2015.

[21] D. Ronan and M. O'Malley, "A new approach to quantify reserve demand in systems with significant installed wind capacity," *IEEE Trans. Power Syst.*, vol. 20, no. 2, pp. 587–595, May 2005.

[22] H. Bludszuweit, J. A. Dominguez-Navarro, and A. Llombart, "Statistical analysis of wind power forecast error," *IEEE Trans. Power Syst.*, vol. 23, no. 3, pp. 983–991, Aug. 2008.

[23] P. Pinson, "Very short term probabilistic forecasting of wind power with generalized logit-normal distributions," *J. Roy. Statist. Soc.: Series C (Appl. Statist.)*, vol. 61, no. 4, pp. 555–576, 2012.

[24] C. E. Rasmussen and C. K. Williams, *Gaussian Processes for Machine Learning*, vol. 1. Cambridge, MA, USA: MIT Press, 2006.

[25] E. W. Bai, "Prediction error adjusted Gaussian process for nonlinear nonparametric system identification," *IFAC Proc.*, vol. 45, no. 16, pp. 101–106, 2012.

[26] J. Yan, K. Li, E. Bai, and A. Foley, "Special condition wind power forecasting based on Gaussian Process and similar historical data," *Proc. IEEE Power Energy Soc. General Meeting*, 2015, pp. 1–5.

[27] J. D. Hamilton, *Time Series Analysis*. Princeton, NJ, USA: Princeton Univ. Press, 1994.

[28] A. Girard, "Multiple-step ahead prediction for non-linear dynamic systems–A Gaussian process treatment with propagation of the uncertainty," *Adv. Neural Inf. Process. Syst.*, vol. 15, pp. 529–536, 2002.

[29] J. Yan, K. Li, E. Bai, Z. Yang, and A. M. Foley, "Time series wind power forecasting based on variant Gaussian Process and TLBO," *Neurocomputing*, vol. 189, pp. 135–144, 2016.

[30] T. Gneiting, F. Balabdaoui, and A. E. Raftery, "Probabilistic forecasts, calibration and sharpness," *J. Roy. Statist. Soc.: Series B (Statist. Methodol.)*, vol. 69, pp. 243–268, 2007.